Natural Glycyrrhizic Acid-Tailored Homogeneous Conductive Polyaniline Hydrogel as a Flexible Strain Sensor

Lianjie Zhao, Hao Zhang, Ning Tang, Min-Hui Li, Jun Hu

Natural Phytic Acid-Assisted Polyaniline/Poly(vinyl alcohol) Hydrogel Showing Self-reinforcing Features

Lianjie Zhao,[†] Hao Zhang,[†] Ning Tang,[†] Min-Hui Li,[,‖] and Jun Hu*[,†]*

†Beijing Advanced Innovation Center for Soft Matter Science and Engineering, Beijing University of Chemical Technology, North Third Ring Road 15, Chaoyang District, Beijing 100029, China. E-mail: jhu@mail.buct.edu.cn

‖Chimie ParisTech, PSL University, CNRS, Institut de Recherche de Chimie Paris, 11 rue Pierre et Marie Curie, Paris 75005, France. E-mail: min-hui.li@chimieparistech.psl.eu

ABSTRACT: Polyaniline (PANi) hydrogels that combine advantages of hydrogels and conductive PANi have recently emerged in wearable devices and personal healthcare. Nevertheless, their mechanical performance often gradually degrades after being used for a period, caused by destruction of the inner structures when external forces are applied. Inspired by biological structures with persistent durability, we develop here a phytic acid-assisted polyaniline/poly(vinyl alcohol) hydrogel that shows self-reinforcing features. As a natural product holding plenty of phosphate groups, phytic acid (PA) plays two crucial roles when preparing this hydrogel: 1) aniline is salinized by PA in aqueous solution to promote *in situ* polymerization, making the resulting PANi conductive; 2) PA/PANi particles form hydrogen bonds with poly(vinyl alcohol) (PVA), acting as stress concentration points to induce structure orientation. The optimal PVA/PA/PANi hydrogel displays dark green with

uniform distribution of PA/PANi particles. After experiencing repetitive 4 × 100 stretching at a strain of 10%, the hydrogel exhibits an enhanced fracture strength (20.35 MPa), Young's modulus (22.66 MPa), and toughness (36.24 $MJ \cdot m^{-3}$) compared with original hydrogel. This self-reinforcing feature is mainly attributed to the formation of anisotropic structures fixed by hydrogen bonds between PA/PANi particles and PVA chains upon repetitive external forces. Moreover, anisotropic structures can be disassembled by swelling the post-stretched hydrogel in water, and the swollen hydrogel shows similar self-reinforcing behaviors. The good mechanical durability and reusable characteristics make PVA/PA/PANi hydrogel a reliable strain sensor. This work provides a structural growing-reviving approach for conductive hydrogels with persistent durability.

KEYWORDS: polyaniline hydrogel, self-reinforcing, phytic acid, poly(vinyl alcohol), reusability

INTRODUCTION

Electronically conductive hydrogels (ECH), constructed by conductive fillers (nanocarbons, metal nanoparticles, and polymers) with flexible hydrogel networks, have recently emerged in areas of wearable devices and personal healthcare for their impressive conductive and mechanical properties.[1-3] Compared with other fillers, polyaniline (PANi) owns chain-level electronic conductivity, and its conjugated structure can construct an electrical pathway for delocalized π electrons. Therefore, PANi is one of the most attractive fillers for ECH.[4-6] However, inappropriate interfacial interactions between flexible hydrogel matrix and rigid PANi fillers arising from polarity mismatch often cause large deterioration in mechanical and conductive performance, which hampers the development of elite PANi hydrogels. To solve

this issue, efforts have been made to improve their compatibility with two strategies. The first strategy relies on the exquisite modification of PANi structure to weaken hydrophobicity by using diverse proton dopants or templates.[7-9] The second strategy aims to create hydrophobic microenvironments in hydrophilic hydrogel matrix.[10-12] Notably, despite the advancements achieved by these two strategies, the mechanical performance of PANi hydrogels still severely degrades after a period of use, as vulnerable inner structures and interactions between PANi fillers and hydrogel matrix would be destructed when external forces are applied. Therefore, designing rational structures to endow PANi hydrogels with persistent durability of mechanical performance remains a big challenge.

Compared with synthetic materials, natural organisms always behave with unparalleled mechanical performance under repetitive loadings because of their multiscale hierarchical architectures. For example, muscles autonomously proliferate, reconstruct, and orient fibril structures through the metabolic process, for adapting to external ever-changing mechanical environment.[13-15] These wondrous events inspire researchers to mimic natural principles when designing materials with persistent durability. Gong *et al.*[16] proposed a strategy to fabricate self-growing hydrogels that responded to repetitive mechanical forces through mechanochemical transduction. But the continuous monomer supply inside the hydrogel was required; consequently, the stiffening/strengthening of the hydrogel suffered from limitations due to reaction kinetics and non-ideal conditions. On the other hand, Verduzco *et al.*[17] developed a self-stiffening liquid crystal elastomer (LCE) in response to periodic compressive strains without involvement of chemical reactions. The stiffening behavior was obtained by reorientation of nematic orders in polydomain LCE under extended dynamic

compression. Apparently, the transformation from polydomain to nematic order preferentially perpendicular to compression direction is the key of the self-stiffening of LCE. Other studies show that rigid structures and sufficient dynamic interactions are generally required to produce anisotropic structures by sensing external forces.[18-20]

In this work, by introducing phytic acid (PA)-doped PANi into polyvinyl alcohol (PVA), we developed a new conductive hydrogel (PVA/PA/PANi) that showed self-reinforcing feature. PA is a natural product from plants, and holds plenty of phosphate groups. It presents two unique characteristics when preparing this hydrogel: 1) aniline was salinized by PA in aqueous solution, which promoted *in situ* polymerization to obtain conductive PANi; and 2) rigid PA/PANi particles formed hydrogen bonds with PVA chains, acting as stress concentration points to induce structure orientation by reversible cleavage and reforming of hydrogen bonds under repetitive stretching. As illustrated in Scheme 1, in the presence of PA and ammonium persulfate (APS), aniline was *in situ* polymerized in an aqueous solution of PVA to afford PVA/PA/PANi complex. After centrifuging and compressing, PVA/PA/PANi hydrogel was obtained. The optimal PVA/PA/PANi hydrogel displayed dark green color with uniform distribution of PA/PANi particles. Its fracture strength, Young's modulus, and toughness were 2.26 MPa, 0.60 MPa, and 5.58 $MJ \cdot m^{-3}$, respectively. After repetitive 4 × 100 stretching under a strain of 10%, its fracture strength, Young's modulus, and toughness were largely enhanced to 20.35 MPa, 22.66 MPa, and 36.24 $MJ \cdot m^{-3}$. This self-reinforcing behavior was mainly attributed to the formation of anisotropic structures during repetitive mechanical forces, which were fixed by reformation of hydrogen bonds between rigid PA/PANi particles and PVA chains. Moreover, anisotropic structures could be disassembled by swelling in water,

and the swollen hydrogel showed similar self-reinforcing behaviors upon external mechanical forces. The good mechanical durability and reusable characteristics make PVA/PA/PANi hydrogel a reliable strain sensor with gauge factor (GF) of 1.5. Therefore, inspired by nature this work succeeded in constructing reusable conductive hydrogels that gain strength under external mechanical stimuli, which is beneficial for prolonging lifetime of materials.

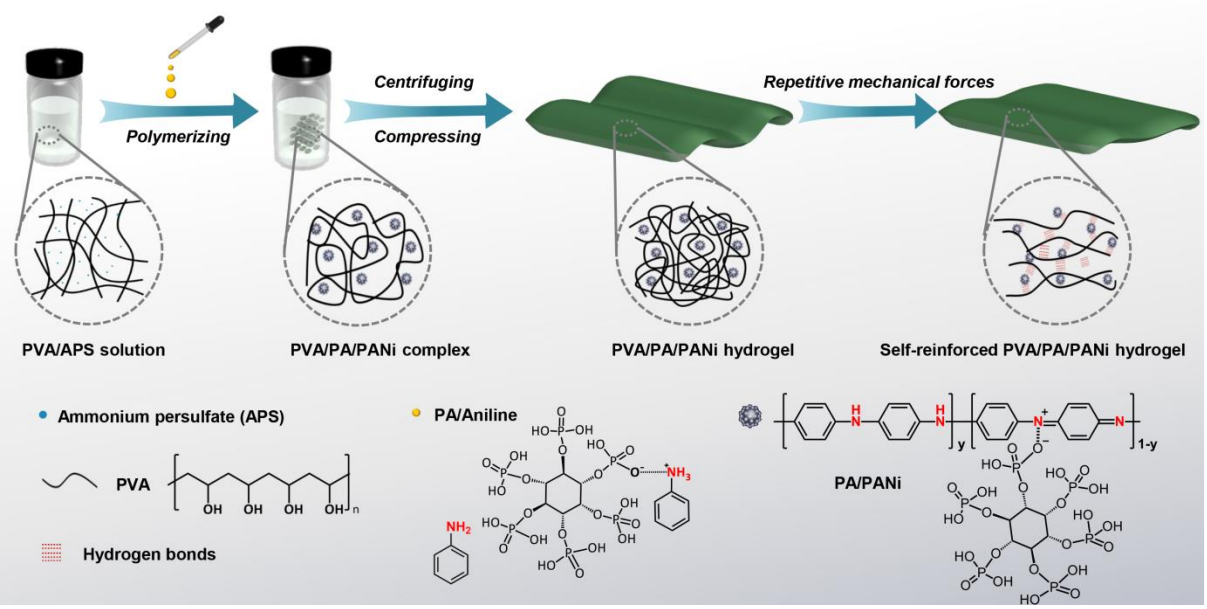

Scheme 1. Schematic illustration of the preparation of PVA/PA/PANi hydrogel showing self-reinforcing feature.

RESULTS AND DISCUSSION

Scheme 1 depicted the consecutive fabrication process of PVA/PA/PANi hydrogel. Typically, aniline was first added into an aqueous solution of PA to get a light yellow solution, which was then dropped into another aqueous solution of PVA and APS at 75°C. After *in situ* polymerization within 2 h at room temperature, the resulting PVA/PA/PANi complex was centrifuged, collected, and compressed in a mold under a pressure of 0.5 kPa for 48 h at room temperature, affording a series of PVA/PA/PANi hydrogels, named as PVA/PA/PANi$_x$, where

x represented the molar ratio of APS to aniline (0%, 10%, 12.5%, and 25%). Under repetitive mechanical forces, PVA chains were stretched in force direction and PA/PANi particles within the hydrogel served as stress concentration points. Consequently, anisotropic orientation of PVA chains was fixed by multiple hydrogen bonds between PVA and PA/PANi particles.

Mechanical properties of the obtained PVA/PA/PANi$_x$ hydrogels were then investigated. Their tensile stress-strain curves showed that with the increase of APS/Aniline ratio from 0% to 25%, both fracture strength and elongation at break increased first yet decreased subsequently (Figure 1a). The maximum values of fracture strength (2.26 MPa), elongation at break (751%), and toughness (5.58 MJ·m^{-3}) have been achieved for PVA/PA/PANi$_{12.5\%}$ hydrogel (Figure 1b). The variation in mechanical performance was attributed to micro-phase interactions between PA/PANi particles and PVA chains. When the APS content was 0%, the hydrogel was transparent and slightly yellow, and its surface was smooth without any particles due to the absence of PANi (Figure 1c and S1a). As the APS content increased to 10%, the hydrogel color changed to green with heterogeneous distribution of colors and a few of PA/PANi particles visible (Figure 1d and S1b). On the contrary, a homogeneous dark green hydrogel was obtained with a roughly uniform distribution of PA/PANi particles around ~0.79 μm when the APS content was 12.5% (Figure 1e, S1c and S2). Further increasing the APS content to 25%, PA/PANi particles aggregated within the hydrogel (Figure 1f and S1d). Apparently, PVA/PA/PANi$_{12.5\%}$ hydrogel with good deformability and high strength possessed appropriate size and distribution of PA/PANi particles, which offered the strongest interactions with PVA matrix for the comprehensive mechanical properties (Figure 1g). Rheological tests further proved this enhanced interfacial interaction between PA/PANi

particles and PVA matrix, as PVA/PA/PANi$_{12.5\%}$ hydrogel performed a dominant storage modulus *G'* (24.99 kPa) over PVA/PA/Aniline hydrogel (14.62 kPa) (Figure S3).

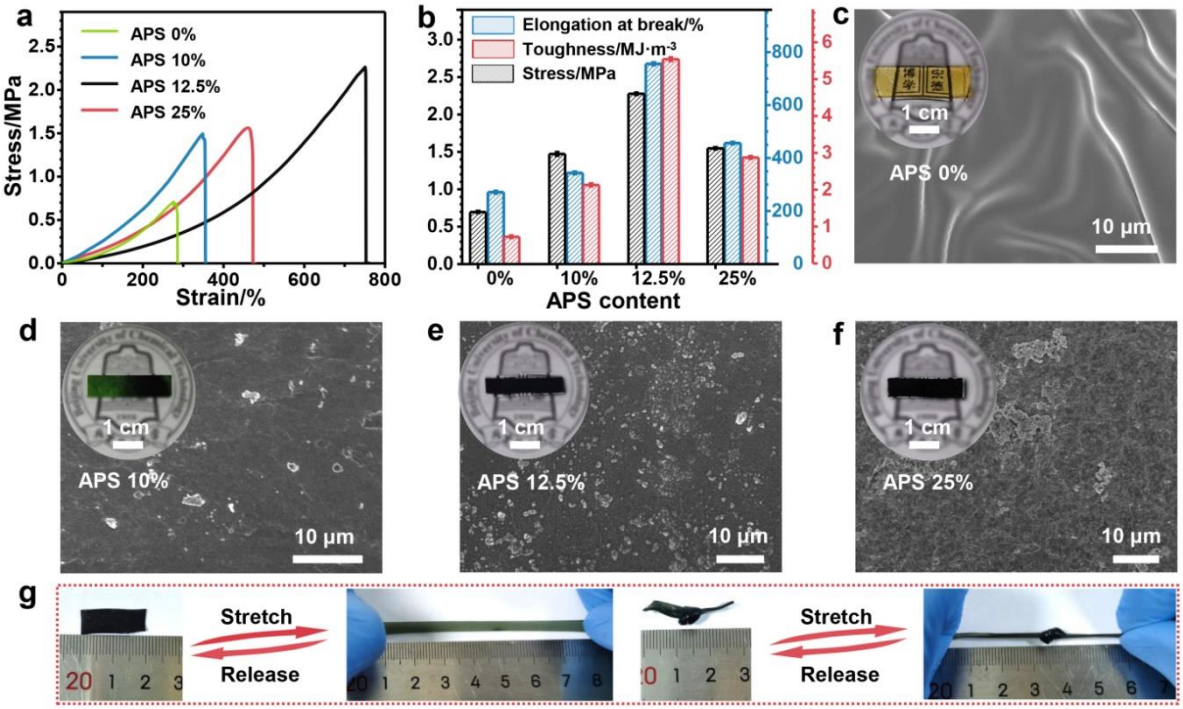

Figure 1. (a) Tensile stress-strain curves of PVA/PA/PANi hydrogel with different APS contents, and (b) the corresponding values of fracture strength, elongation at break, and toughness. Scanning electron microscope (SEM) images of the surface of PVA/PA/PANi hydrogel with the APS content of (c) 0%, (d) 10%, (e) 12.5%, and (f) 25%. Insets in (c-f) were digital photos of the hydrogels. (g) Digital photos of PVA/PA/PANi$_{12.5\%}$ hydrogel in a regular stretching and a twisted stretching state.

Scanning electron microscope-energy dispersive spectroscopy (SEM-EDS) showed that the relative contents of C, O, N, and P elements of PVA/PA/PANi$_{12.5\%}$ hydrogel were 43.24%, 46.94%, 1.47%, and 8.35% (Figure S4), respectively, consistent with the hydrogel formulation. The corresponding mapping results demonstrated that C, O, and N were evenly distributed on hydrogel surface (Figure 2a-c), indicative of successful synthesis of PANi.[21,22]

In contrast, element P was concentrated on PA/PANi particles due to electrostatic interactions between PA and PANi (Figure 2d).[23] As for PVA/PA/PANi$_{25\%}$, the local rich-distribution of P and N clearly revealed the aggregation structure of PA/PANi particles in hydrogel (Figure S5). Element compositions of PVA/PA/PANi$_{12.5\%}$ hydrogel were further detected by X-ray photoelectron spectroscopy (XPS), where P2p, C1s, N1s, and O1s were located at 153.1, 285.1, 400.1, and 532.1 eV, respectively (Figure 2e). The high-resolution XPS in O1s region could be divided into three electronic states at 531.7, 532.3, and 533.3 eV, corresponding to P=O, P−O, and C−O (Figure 2f),[24,25] while P2p region was resolved into two peaks at 133.4 (P=O···H−O−P) and 134.1 eV (P=O···H−O−C), revealing the existence of inter- and intra-molecular hydrogen bonds between PA and PVA (Figure 2g).[26,27] Moreover, benzenoid amine (−NH−) at 399.6 eV, protonated imine (−NH^+=) at 400.1 eV, and benzenoid unit (−NH_2^+−) at 401.7 eV were observed in high-resolution N1s spectrum (Figure 2h), verifying the conductive emeraldine-salt form of PANi doped by proton acid.[28,29] Furthermore, PVA/PA/PANi$_{12.5\%}$ hydrogel exhibited two absorption peaks at 401 and 786 nm in UV-Vis spectrum (Figure 2i), which were assigned to π-π* transition of benzenoid rings and exciton absorption of quinoid rings, again indicating its conductive nature.[8,30] After integrating PVA/PA/PANi$_{12.5\%}$ hydrogel into a circuit, a light-emitting diode (LED) was lit upon turning on the switch (inset, Figure 2i), and its conductivity was measured to be 0.31 S·m^{-1}, higher than that of PVA/PA/PANi hydrogels with other APS content (Figure S6).

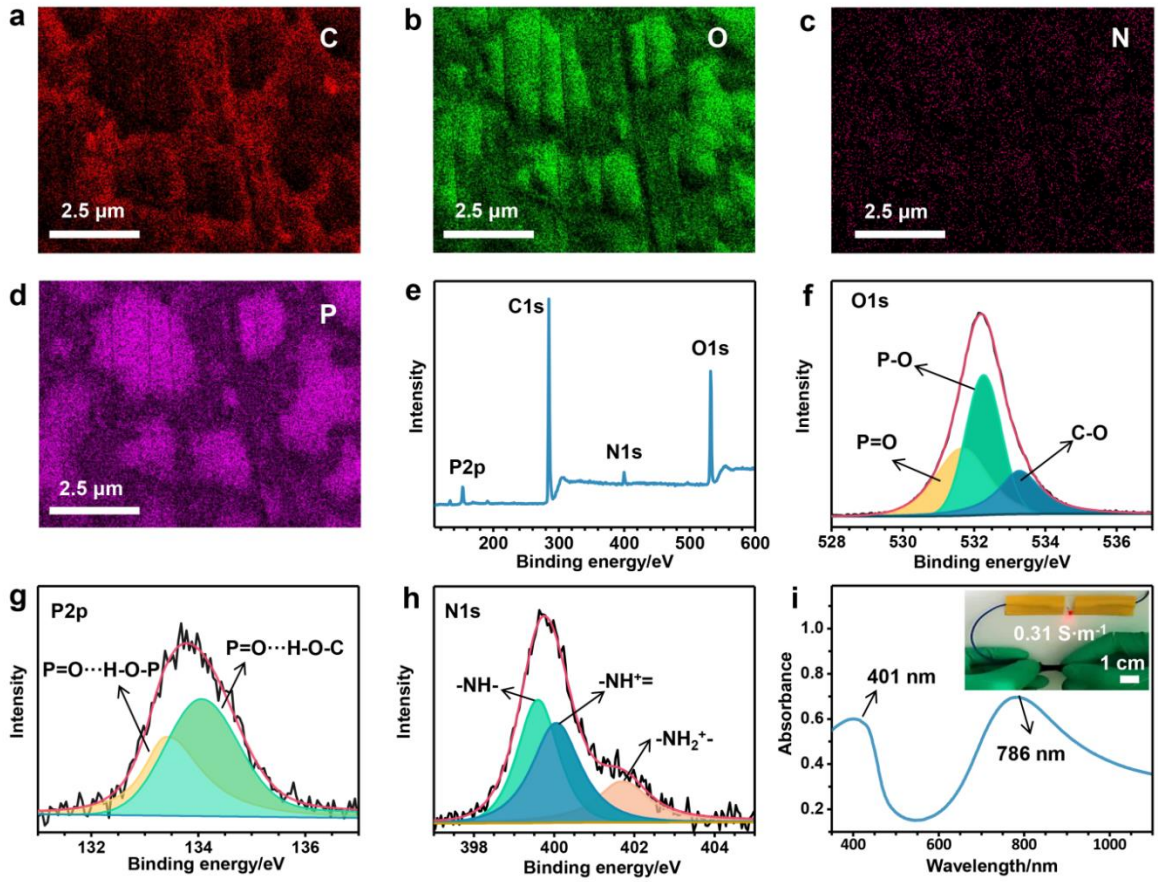

Figure 2. SEM-mapping of the surface of PVA/PA/PANi$_{12.5\%}$ hydrogel with element distribution of (a) C, (b) O, (c) N, and (d) P. (e) X-ray photoelectron spectroscopy (XPS) of PVA/PA/PANi$_{12.5\%}$ hydrogel, and the corresponding high-resolution spectroscopy of (f) O1s, (g) P2p, and (h) N1s. (i) UV-Vis spectrum of PVA/PA/PANi$_{12.5\%}$ hydrogel from 350 to 1100 nm. Inset showed the hydrogel conductivity in a circuit with a light-emitting diode.

Most hydrogels often suffer from gradual decay of mechanical performance during their long-term usage. Intriguingly, a rising mechanical signal of PVA/PA/PANi$_{12.5\%}$ hydrogel was observed in durability test. The tensile strength increased from 0.06 to 1.43 MPa at a strain of 10% after repetitive 4 × 100 stretching cycles (Figure 3a and S7), strongly revealing a self-reinforcing feature of the hydrogel. As a result, the post-stretched PVA/PA/PANi$_{12.5\%}$ hydrogel exhibited an enhanced mechanical performance (Figures 3b), that is, fracture

strength, Young's modulus, and toughness were 20.35 MPa, 22.66 MPa, and 36.24 $MJ \cdot m^{-3}$, respectively, much higher than those of original hydrogel (Figures 3c). To further prove this self-reinforcing feature, three consecutive tests of PVA/PA/$PANi_{12.5\%}$ hydrogel under a strain from 20% to 50% were investigated. As displayed in Figure 3d and S8, the tensile strength was improved to 1.98, 2.91, 3.44, and 4.59 MPa from 0.22, 0.42, 0.66, and 1.03 MPa, respectively, when a strain of 20%, 30%, 40%, and 50% was applied, indicating that the self-reinforcing behaviors remained under different strains. The corresponding mechanical hysteresis curves during consecutive tests were shown in Figure S9. The hysteresis loop gradually increased with cyclic numbers, and the dissipated energy (ΔU) at a strain of 20%, 30%, 40%, and 50% were 0.16, 0.32, 0.61, and 1.13 $MJ \cdot m^{-3}$ in the third cycle, higher than those in the first cycle. The increasing ΔU uncovered the fact that the density of sacrificial hydrogen bonds rose gradually during cyclic stretches.[31,32] In addition, the experiments of crack tolerance and puncture resistance solidly confirmed the reinforcement. In crack tolerance tests, the fracture strength of the post-stretched hydrogel with a notch reached 8.86 MPa accompanied with a fracture energy of 75.66 $kJ \cdot m^{-2}$, much larger than those of original hydrogel (0.51 MPa and 4.58 $kJ \cdot m^{-2}$) (Figure S10). While in puncture resistance tests, the post-stretched hydrogel could withstand a force as high as 11.16 N at the needle displacement of 4.94 mm, better than those of original hydrogel (1.58 N at 4.53 mm) (Figure S11).

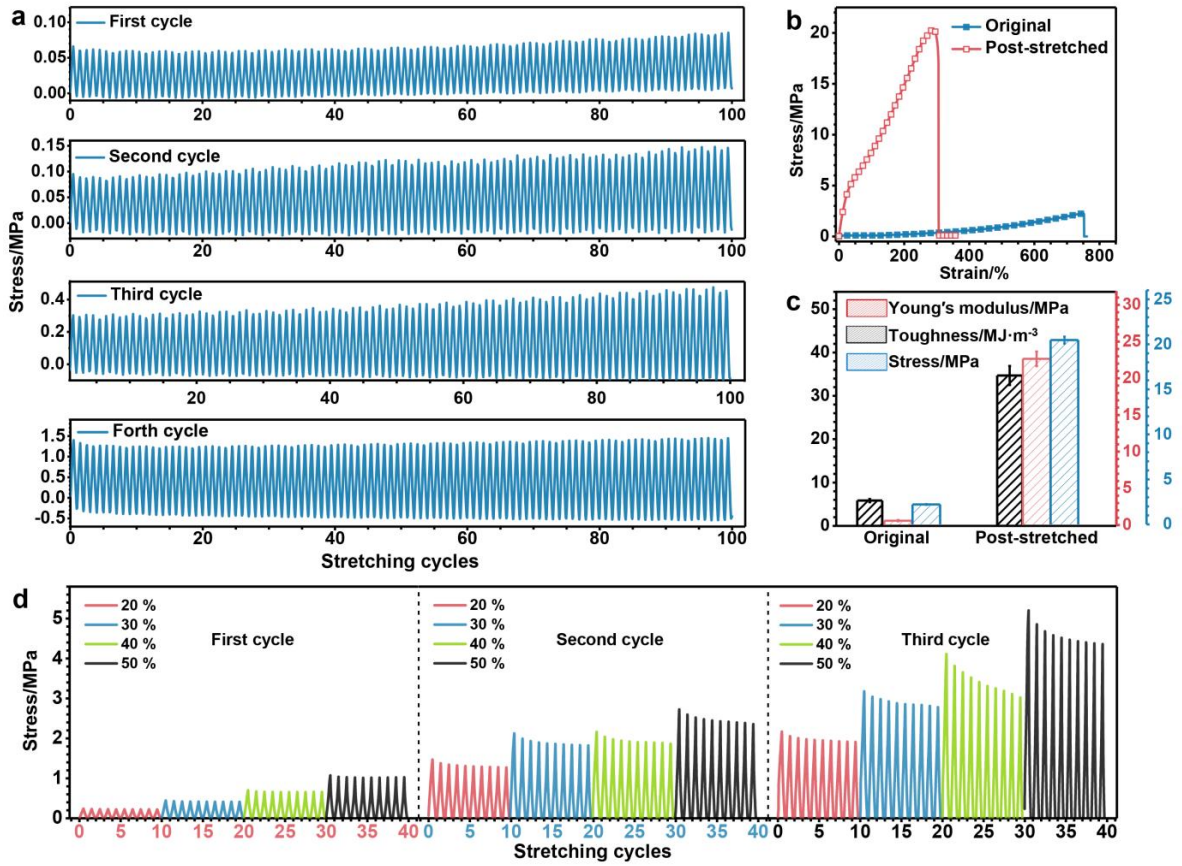

Figure 3. (a) Tensile strength of PVA/PA/PANi$_{12.5\%}$ hydrogel at a strain of 10% during repetitive 4 × 100 stretching cycles with a ten-minute interval. (b) Tensile stress-strain curves, and (c) the corresponding values of fracture strength, Young's modulus, and toughness of original and post-stretched PVA/PA/PANi$_{12.5\%}$ hydrogel. (d) Tensile strength of PVA/PA/PANi$_{12.5\%}$ hydrogel at a strain from 20% to 50% for three consecutive tests with a 10-minute interval.

As the mechanical performance of materials primarily relied on their inner structures, SEM images were firstly used to validate microstructures of PVA/PA/PANi$_{12.5\%}$ hydrogel after stretching. As shown in Figure 4a, the aligned structures along axial direction were observed clearly both on surface and cross-section of the post-stretched hydrogel in comparison with isotropic structures of original hydrogel. It indicated that the self-reinforcing behavior was

mainly promoted by formation of anisotropic structures, during which randomly distributed PVA segments progressively re-oriented and aligned toward direction of the applied stretches. The movement of PVA segments was further confirmed by differential scanning calorimeter (DSC). Figure 4b displayed that the glass transition temperature (T_g) of hydrogel increased to 46.4 from 41.7°C after formation of anisotropic structures. Understandably, the oriented structures hindered the mobility of PVA segments and raised activation energy for glass transition. Moreover, the melting temperature (T_m) of PVA rose from 194.9 to 198.5°C with a growing melting enthalpy from 4.2 to 5.3 $J \cdot g^{-1}$. Concerning the reported enthalpy value of fusion for 100% crystalline PVA,[33,34] the crystallinity was deduced to be 15.9% and 20.1% for PVA/PA/PANi$_{12.5\%}$ hydrogel before and after cyclic stretching (Figure S12). This improved crystallinity demonstrated an enhanced intermolecular hydrogen bonds between PVA chains in anisotropic structures of post-stretched hydrogel. Fourier transform infrared spectroscopy (FTIR) spectra provided more evidence for the variation of hydrogen bonds. The stretching vibration of hydroxyl groups shifted from 3228 to 3258 cm^{-1} when anisotropic structures formed in post-stretched hydrogel (Figure 4c and S13), revealing an increase of intermolecular hydrogen bonds.[35,36] In addition, X-ray diffraction (XRD) showed that a relatively sharper signal was obtained for the post-stretched hydrogel, although peaks at 2θ of 19.6° and 41.1° corresponding to (101) and (102) planes of PVA crystallites were observed for both hydrogels (Figure S14),[37,38] verifying a better crystallinity of the post-stretched hydrogel. More evidences came from small angle X-ray scattering (SAXS) profiles, where the post-stretched hydrogel exhibited a peak with a smaller distance of adjacent crystalline domains (0.09 $Å^{-1}$, 6.98 nm), in sharp contrast to the weak shoulder peak of original hydrogel

(Figure S15). The difference in crystallinity could also be observed intuitively by polarizing optical microscopy, with birefringence in post-stretched hydrogel, but not original hydrogel (Figure S16).

To clarify the formation mechanism of the oriented structures in depth, a method of DCC (drying in confined conditions) was used under 0% pre-strain. In general, during the DCC process hydrogels were stretched along the length direction because of anisotropic contraction, thus generating the contraction stress in axial direction.[18,19] As shown in Figure 4d, the axial contraction stress of PVA/PA/PANi$_{12.5\%}$ hydrogel increased gradually at initial stage I (before 0.5 h) but rose abruptly at transition stage II (0.5-1.8 h). After that, its growth slowed down at the final stage III (after 1.8 h). It was postulated that the increased stress at initial stage I was related to rubber elasticity of PVA chains, while at transition stage II the rigid PA/PANi particles acting as stress concentration points induced PVA to form oriented structures, because rigid components were normally necessary for sensing mechanical signal to create hierarchical architectures.[18] For comparison, a control hydrogel of PVA/PA/Aniline that lacked rigid particles was prepared. Its axial contraction stress just increased smoothly without any transition stage, and no self-reinforcing phenomenon was observed during the 4 × 100 stretching cycles (Figure S17). After stretching, there was no aligned structures on its surface and cross-section (Figure S18). These results indicated that rigid particles and water evaporation played crucial roles in the self-reinforcing process. As illustrated in Figure 4e, the majority of PVA chains remained amorphous in original hydrogel. Once the stretch was applied, rigid PA/PANi particles connected robustly with PVA matrix, which served as stress concentration points to withstand external force and convert environmental cues into

mechanical motions. Consequently, anisotropic structures were generated and fixed by hydrogen bonds between PA/PANi particles and PVA matrix. At the same time, water evaporation and aligned structures would navigate PVA to experience more hydrogen bonds, which further contributed to anchorage of the acquired structures. As a result, the hydrogel with anisotropic structures and improved mechanical performance formed as the number of stretches increased.

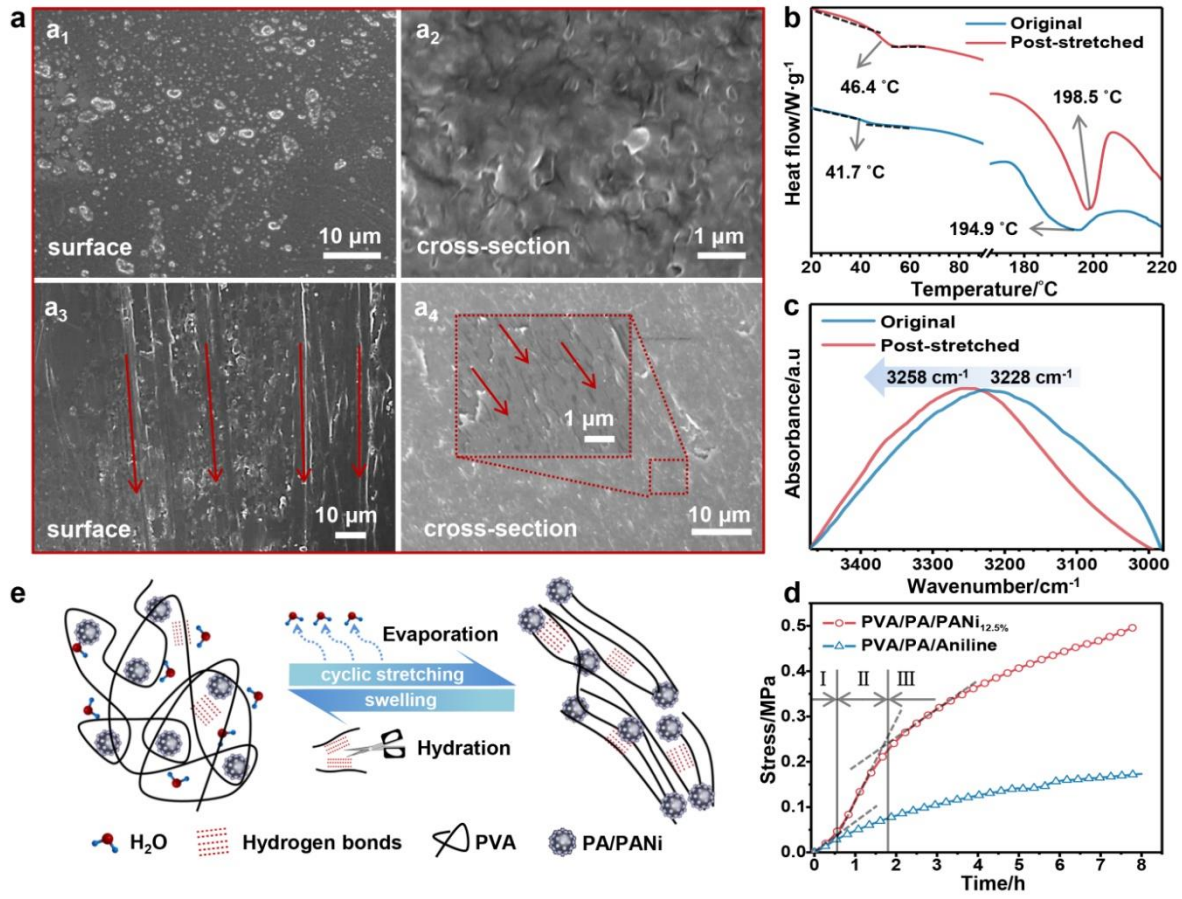

Figure 4. (a) SEM images of the surface and cross-section of original (a_1, a_2) and post-stretched (a_3, a_4) PVA/PA/PANi$_{12.5\%}$ hydrogel. The arrow direction meant the aligned structures along stretching direction. (b) Differential scanning calorimeter (DSC) of original and post-stretched PVA/PA/PANi$_{12.5\%}$ hydrogel in temperature range from 20 to 220 °C with a heating rate of 5 °C·min^{-1} under N_2 atmosphere. (c) FTIR spectra of original and

post-stretched PVA/PA/PANi$_{12.5\%}$ hydrogels in wavenumber range from 2980 to 3480 cm^{-1}. (d) Stress variation of PVA/PA/PANi$_{12.5\%}$ and PVA/PA/Aniline hydrogels under 0% pre-strain during the DCC process. (e) The proposed formation mechanism of anisotropic structures with the improved mechanical performance.

It is known that water is a good plasticizer for PVA chains and can disrupt hydrogen bonds among PVA chains to produce lubrication effect.[39,40] Therefore, anisotropic structures of the post-stretched hydrogel could return to original states after swelling in water (Figure 4e), which is beneficial for material recycling. As shown in Figure 5a, after immersing the post-stretched PVA/PA/PANi$_{12.5\%}$ hydrogel in water for 24 h, the swollen hydrogel behaved a maximum fracture strength of 1.41 MPa with elongation at break of 690%, which recovered to 62% of fracture strength of original hydrogel. Notably, the mechanical properties of hydrogels heavily relied on swelling ratio.[41-43] As shown in Figure S19, with prolonging the immersing time, the swelling ratio increased to 177% at 5 min, 254% at 15 min, and reached the equilibrium of 280% after 60 min. Accordingly, the fracture strength of post-stretched PVA/PA/PANi$_{12.5\%}$ hydrogel decreased to 12.08, 4.67, and 1.40 MPa, respectively. SEM image showed that the swollen hydrogel had isotropic structures with uniform distributions of PA/PANi particles (Figure 5b), similar to original PVA/PA/PANi$_{12.5\%}$ hydrogel. XRD patterns in Figure 5c revealed that the peak corresponding to (101) plane of PVA crystalline shifted from 19.6˚ to 24.3˚, revealing an increased inter-planar distance between PVA segments. The weakened peak sharpness was due to the deconstruction of crystalline domains under the swelling operation.[44] Moreover, the swollen hydrogel still maintained the self-reinforcing property. As shown in Figure 5d, a self-reinforcing phenomenon was observed during two

consecutive tensile tests with a strain from 20% to 50%. In detail, the tensile strength was improved to 0.26, 0.46, 0.85, and 1.46 MPa from 0.08, 0.13, 0.19, and 0.29 MPa, respectively, when a strain of 20%, 30%, 40%, and 50% was applied (Figure S20), which indicated that the self-reinforcing were reproducible after swelling operation to the post-stretched hydrogel. Coincident with the self-reinforcing process in Figure 4e, rigid PA/PANi particles bonded with PVA would perceive the stress under deformation. As a result, anisotropic structures showing the improved mechanical performance gradually generated again induced by PA/PANi particles and fixed by the new-formed hydrogen bonds.

In addition to self-reinforcing and reusable features, PVA/PA/PANi$_{12.5\%}$ hydrogel also displayed electrical conductivity, attributing to the movement of delocalized electrons and hopping electrons between adjacent redox sites on PANi. The physical operations such as stretching and compressing would influence the electronic transmission distance, resulting in resistance change of the hydrogel. In a circuit integrating PVA/PA/PANi$_{12.5\%}$ hydrogel with a LED, the brightness of LED darkened upon stretching hydrogel to 300%, demonstrating a fast response in resistance to the applied strain (inset, Figure 5e). When PVA/PA/PANi$_{12.5\%}$ hydrogel was utilized to detect strain changes from 0% to 300%, a stable sensitivity with gauge factor (GF) of 1.5 and a good linear fitting of resistance variation were obtained (Figure 5e). Despite the self-reinforce capability the GF of post-stretched hydrogel was same as the original one (Figure S21), because the negligible shape change during stretching ensured the conductive pathway stable.[45,46] Figure 5f showed the strain sensing under cyclic tensile tests with different strains (10−50%), where relative resistance change (ΔR:R_0) was 2.7%, 12.0%, 33.5%, 46.5%, and 63.1%, respectively, under a strain of 10%, 20%, 30%, 40%,

and 50%. When applied to detect durable performance under a period of strains, the resistance rapidly increased with the stretching extent and displayed a step-by-step resistance change with negligible hysteresis (Figure 5g). Furthermore, PVA/PA/PANi$_{12.5\%}$ hydrogel could sense motions of wrist, elbow, and knee (Figure 5h). During the bending and extension of joints, the hydrogel was stretched and the resistance was recorded. The change of resistance increased as the bending amplitude, indicating good sensitivity and stability of the hydrogel.

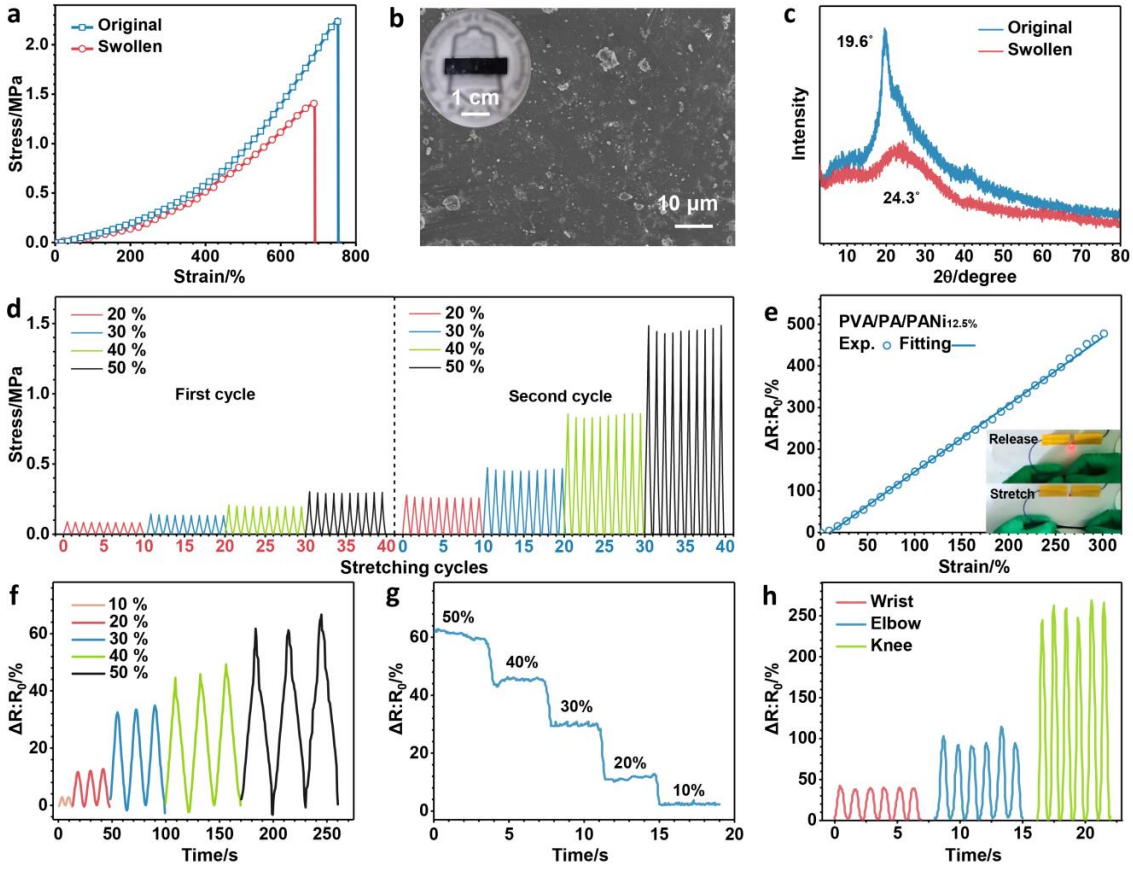

Figure 5. (a) Tensile stress-strain curves of the swollen and the original PVA/PA/PANi$_{12.5\%}$ hydrogel. (b) SEM image of the surface of the swollen PVA/PA/PANi$_{12.5\%}$ hydrogel. Inset was a digital photo of the swollen hydrogel. (c) X-ray diffraction (XRD) of the swollen and the original PVA/PA/PANi$_{12.5\%}$ hydrogel in 2θ range from 4 to 80° with a scan rate of 10°·min^{-1}.

(d) Tensile strength of the swollen PVA/PA/PANi$_{12.5\%}$ hydrogel under a strain from 20% to 50% for two consecutive tests with a 10-minute interval. (e) Relative resistance change of PVA/PA/PANi$_{12.5\%}$ hydrogel as a function of tensile strain from 0% to 300%. Inset showed the brightness of LED before and after stretching hydrogel. Relative resistance change (f) under repetitive strains and (g) in the stepped stretching from 10% to 50% strain. (h) Sensing performance in monitoring electric signal variations to human joint movements.

CONCLUSION

In summary, inspired by biological structures with persistent durability, we have fabricated a series of conductive PVA/PA/PANi hydrogels composed of PA-doped PANi and PVA matrix. By optimizing APS content for achieving uniform distribution of PA/PANi particles within PVA matrix, the optimal PVA/PA/PANi$_{12.5\%}$ hydrogel exhibited good mechanical property with fracture strength of 2.26 MPa and elongation at break of 751%. Intriguingly, PVA/PA/PANi$_{12.5\%}$ hydrogel showed self-reinforcing features when external forces were applied. For example, after experiencing repetitive 4×100 stretching at a strain of 10%, PVA/PA/PANi$_{12.5\%}$ hydrogel showed an enhanced fracture strength of 20.35 MPa, Young's modulus of 22.66 MPa, and toughness of 36.24 MJ·m^{-3}, respectively, much higher than those before stretching. The formation of anisotropic structures fixed by hydrogen bonds between rigid PA/PANi particles and PVA chains was revealed as the key factor during this self-reinforcing process. In addition, anisotropic structures could be reset after swelling the post-stretched hydrogel in water due to the plasticization effect of water molecules on PVA. The swollen hydrogel exhibited similar mechanical self-reinforcing feature under repetitive stretching. The good mechanical durability and reusable characteristics make

PVA/PA/PANi$_{12.5\%}$ hydrogel a reliable strain sensor with GF of 1.5. Compared with other reported hydrogels having similar compositions or reinforcement features, the resettable structure conferred our conductive hydrogel with reusable self-reinforced property (Table S1), which might pave the way for developing functional hydrogels with the prolonged lifetime.

EXPERIMENTAL SECTION

Preparation of PVA/PA/PANi hydrogel. Generally, aniline (An, 0.141 mL, 1.5 mmol) was first added into 3 mL aqueous solution of phytic acid (PA, 3 mmol) to afford a light yellow aqueous solution. This solution was then dropped slowly into 10 mL aqueous solution of polyvinyl alcohol (PVA, 0.5 g) and ammonium persulfate (APS, 42 mg, 0.19 mmol) at 75 °C under stirring, resulting in the formation of PVA/PA/Aniline complex that *in situ* polymerized into PVA/PA/PANi within 2 h at room temperature. After centrifuging at a rotation speed of 8000 r/min for 30 min, PVA/PA/PANi complex was collected and compressed in a mold (2 cm × 8 cm × 0.1 cm) under a pressure of 0.5 kPa for 48 h at room temperature, consequently affording PVA/PA/PANi$_{12.5\%}$ hydrogel. Other PVA/PA/PANi hydrogels with different APS contents (10%, 25%, and 50%) and the control hydrogel of PVA/PA/Aniline without APS were prepared similarly.

ASSOCIATED CONTENT

Supporting Information. The Supporting Information is available free of charge. TEM images of PA/PANi with different APS contents (Figure S1); size distribution of PA/PANi particles in PVA/PA/PANi$_{12.5\%}$ hydrogel (Figure S2); frequency-dependent storage modulus G' and loss modulus G'' of PVA/PA/Aniline and PVA/PA/PANi$_{12.5\%}$ hydrogel (Figure S3); SEM-EDS of the surface of PVA/PA/PANi$_{12.5\%}$ hydrogel (Figure S4); SEM-EDS mapping of

the surface of PVA/PA/PANi$_{25\%}$ hydrogel (Figure S5); conductivity of PVA/PA/PANi hydrogels with different APS contents (Figure S6); tensile strength of PVA/PA/PANi$_{12.5\%}$ hydrogel at a strain of 10% during cyclical tests (Figure S7); tensile strength of PVA/PA/PANi$_{12.5\%}$ hydrogel at a progressive strain during cyclical tests (Figure S8); cyclic loading-unloading curves of PVA/PA/PANi$_{12.5\%}$ hydrogel at a progressive strain (Figure S9); crack tolerance (Figure S10), puncture resistance (Figure S11), crystallinity and melting enthalpy (Figure S12), FTIR (Figure S13), XRD (Figure S14), SAXS (Figure S15) and POM images (Figure S16) of original and post-stretched PVA/PA/PANi$_{12.5\%}$ hydrogel; cyclic tensile tests of PVA/PA/Aniline hydrogel at a strain of 10% (Figure S17); SEM images of post-stretched PVA/PA/Aniline hydrogel (Figure S18); relationship between swelling ratio and mechanical property of post-stretched hydrogel (Figure S19); tensile strength of swollen PVA/PA/PANi$_{12.5\%}$ hydrogel at a progressive strain during cyclical tests (Figure S20); GF of post-stretched hydrogel (Figure S21).

AUTHOR INFORMATION

Corresponding Author

*E-mail: jhu@mail.buct.edu.cn (Jun Hu)

*E-mail: min-hui.li@chimieparistech.psl.eu (Min-Hui Li)

Author Contributions

L.Z., M.L., and J.H. developed the concept and designed the experiment. L.Z., H.Z., and N.T. characterized the materials. L.Z. interpreted the results and drafted the article with inputs from all authors. J.H. funded and supervised the project. M.L and J.H. revised the manuscript. All authors have given approval to the final version of the manuscript.

Notes

The authors declare no competing financial interest.

ACKNOWLEDGMENT

This work is supported by the Open Fund of Anhui Province Key Laboratory of Environment-friendly Polymer Materials, and National Key Laboratory of Science and Technology on Advanced Composite (KZ42191814).

REFERENCES

(1) Talebian, S.; Mehrali, M.; Taebnia, N.; Pennisi, C. P.; Kadumudi, F. B.; Foroughi, J.; Hasany, M.; Nikkhah, M.; Akbari, M.; Orive, G.; Dolatshahi-Pirouz, A. Self-Healing Hydrogels: The Next Paradigm Shift in Tissue Engineering? *Adv. Sci.* **2019**, *6*, 1801664.

(2) Hu, C.; Zhang, Y.; Wang, X.; Xing, L.; Shi, L.; Ran, R. Stable, Strain-Sensitive Conductive Hydrogel with Antifreezing Capability, Remoldability, and Reusability. *ACS Appl. Mater. Interfaces* **2018**, *10*, 44000-44010.

(3) Zhou, H.; Wang, Z.; Zhao, W.; Tong, X.; Jin, X.; Zhang, X.; Yu, Y.; Liu, H.; Ma, Y.; Li, S.; Chen, W. Robust and Sensitive Pressure/Strain Sensors from Solution Processable Composite Hydrogels Enhanced by Hollow-Structured Conducting Polymers. *Chem. Eng. J.* **2021**, *403*, 126307.

(4) Han, X.; Xiao, G.; Wang, Y.; Chen, X.; Duan, G.; Wu, Y.; Gong, X.; Wang, H. Design and Fabrication of Conductive Polymer Hydrogels and Their Applications in Flexible Supercapacitors. *J. Mater. Chem. A* **2020**, *8*, 23059-23095.

(5) Ma, Z.; Shi, W.; Yan, K.; Pan, L.; Yu, G. Doping Engineering of Conductive Polymer Hydrogels and Their Application in Advanced Sensor Technologies. *Chem. Sci.* **2019**, *10*,

6232-6244.

(6) Li, P.; Jin, Z.; Peng, L.; Zhao, F.; Xiao, D.; Jin, Y.; Yu, G. Stretchable All-Gel-State Fiber-Shaped Supercapacitors Enabled by Macromolecularly Interconnected 3D Graphene/Nanostructured Conductive Polymer Hydrogels. *Adv. Mater.* **2018**, *30*, 1800124.

(7) Shen, Y.; Qin, Z.; Li, T.; Zeng, F.; Chen, Y.; Liu, N. Boosting the Supercapacitor Performance of Polyaniline Nanofibers through Sulfonic Acid Assisted Oligomer Assembly During Seeding Polymerization Process. *Electrochim. Acta* **2020**, *356*, 136841.

(8) Han, J.; Ding, Q.; Mei, C.; Wu, Q.; Yue, Y.; Xu, X. An Intrinsically Self-Healing and Biocompatible Electroconductive Hydrogel Based on Nanostructured Nanocellulose-Polyaniline Complexes Embedded in A Viscoelastic Polymer Network Towards Flexible Conductors and Electrodes. *Electrochim. Acta* **2019**, *318*, 660-672.

(9) Gan, D.; Shuai, T.; Wang, X.; Huang, Z.; Ren, F.; Fang, L.; Wang, K.; Xie, C.; Lu, X. Mussel-Inspired Redox-Active and Hydrophilic Conductive Polymer Nanoparticles for Adhesive Hydrogel Bioelectronics. *Nano-Micro Lett.* **2020**, *12*, 169.

(10) Peng, Q.; Chen, J.; Wang, T.; Peng, X.; Liu, J.; Wang, X.; Wang, J.; Zeng, H. Recent Advances in Designing Conductive Hydrogels for Flexible Electronics. *InfoMat* **2020**, *2*, 843-865.

(11) Gong, Q.; Li, Y.; Liu, X.; Xia, Z.; Yang, Y. A Facile Preparation of Polyaniline/Cellulose Hydrogels for All-in-One Flexible Supercapacitor with Remarkable Enhanced Performance. *Carbohydr. Polym.* **2020**, *245*, 116611.

(12) Li, W.; Li, X.; Zhang, X.; Wu, J.; Tian, X.; Zeng, M.; Qu, J.; Yu, Z. Flexible Poly(vinyl alcohol)-Polyaniline Hydrogel Film with Vertically Aligned Channels for an Integrated and

Self-Healable Supercapacitor. *ACS Appl. Energy Mater.* **2020**, *3*, 9408-9416.

(13) Phillips, S. M. Protein Requirements and Supplementation in Strength Sports. *Nutrition* **2004**, *20*, 689-695.

(14) Phillips, S. M. A Brief Review of Higher Dietary Protein Diets in Weight Loss: A Focus on Athletes. *Sports Med.* **2014**, *44*, S149-S153.

(15) Wolfe, R. R. Protein Supplements and Exercise. *Am. J. Clin. Nutr.* **2000**, *72*, 551S-557S.

(16) Matsuda, T.; Kawakami, R.; Namba, R.; Nakajima, T.; Gong, J. Mechanoresponsive Self-Growing Hydrogels Inspired by Muscle Training. *Science* **2019**, *363*, 504-508.

(17) Agrawal, A.; Chipara, A. C.; Shamoo, Y.; Patra, P. K.; Carey, B. J.; Ajayan, P. M.; Chapman, W. G.; Verduzco, R. Dynamic Self-Stiffening in Liquid Crystal Elastomers. *Nat. Commun.* **2013**, *4*, 1739.

(18) Mredha, M. T. I.; Guo, Y.; Nonoyama, T.; Nakajima, T.; Kurokawa, T.; Gong, J. A Facile Method to Fabricate Anisotropic Hydrogels with Perfectly Aligned Hierarchical Fibrous Structures. *Adv. Mater.* **2018**, *30*, 1704937.

(19) Mredha, M. T. I.; Le, H. H.; Tran, V. T.; Trtik, P.; Cui, J.; Jeon, I. Anisotropic Tough Multilayer Hydrogels with Programmable Orientation. *Mater. Horiz.* **2019**, *6*, 1504-1511.

(20) Meng, Y.; Zhao, X.; Ye, L. Construction of Dual Orientation Crystalline Structure in Poly(vinyl alcohol)/Graphene Oxide Nano-Composite Hydrogels and Reinforcing Mechanism. *Ind. Eng. Chem. Res.* **2019**, *58*, 10908-10921.

(21) He, Y.; Pan, D.; Chi, H.; Luo, F.; Jiang, Y.; Ge, D.; Bai, H. Continuous and Patterned Conducting Polymer Coatings on Diverse Substrates: Rapid Fabrication by Oxidant-Intermediated Surface Polymerization and Application in Flexible Devices. *ACS*

Appl. Mater. Interfaces **2021**, *13*, 5583-5591.

(22) Zornitta, R. L.; Ruotolo, L. A. M.; de Smet, L. C. P. M. High-Performance Carbon Electrodes Modified with Polyaniline for Stable and Selective Anion Separation. *Sep. Purif. Technol.* **2022**, *290*, 120807.

(23) Su, G.; Yin, S.; Guo, Y.; Zhao, F.; Guo, Q.; Zhang, X.; Zhou, T.; Yu, G. Balancing the Mechanical, Electronic, and Self-Healing Properties in Conductive Self-Healing Hydrogel for Wearable Sensor Applications. *Mater. Horiz.* **2021**, *8*, 1795-1804.

(24) Liu, X.; Zou, S.; Liu, K.; Lv, C.; Wu, Z.; Yin, Y.; Liang, T.; Xie, Z. Highly Compressible Three-Dimensional Graphene Hydrogel for Foldable All-Solid-State Supercapacitor. *J. Power Sources* **2018**, *384*, 214-222.

(25) Kannan, A. G.; Choudhury, N. R.; Dutta, N. K. Synthesis and Characterization of Methacrylate Phospho-Silicate Hybrid for Thin Film Applications. *Polymer* **2007**, *48*, 7078-7086.

(26) Hu, R.; Zhao, J.; Wang, Y.; Li, Z.; Zheng, J. A Highly Stretchable, Self-Healing, Recyclable and Interfacial Adhesion Gel: Preparation, Characterization and Applications. *Chem. Eng. J.* **2019**, *360*, 334-341.

(27) Puziy, A. M.; Poddubnaya, O. I.; Socha, R. P.; Gurgul, J.; Wisniewski, M. XPS and NMR Studies of Phosphoric Acid Activated Carbons. *Carbon* **2008**, *46*, 2113-2123.

(28) Narayanan, A. P.; Unni, K. N. N.; Surendran, K. P. Aerogels of V_2O_5 Nanowires Reinforced by Polyaniline for Electromagnetic Interference Shielding. *Chem. Eng. J.* **2021**, *408*, 127239.

(29) Ballabio, M.; Zhang, T.; Chen, C.; Zhang, P.; Liao, Z.; Hambsch, M.; Mannsfeld, S. C.

B.; Zschech, E.; Sirringhaus, H.; Feng, X.; Bonn, M.; Dong, R.; Cánovas, E. Band-Like Charge Transport in Phytic Acid-Doped Polyaniline Thin Films. *Adv. Funct. Mater.* **2021**, *31*, 2105184.

(30) Lyu, W.; Li, J.; Zheng, L.; Liu, H.; Chen, J.; Zhang, W.; Liao, Y. Fabrication of 3D Compressible Polyaniline/Cellulose Nanofiber Aerogel for Highly Efficient Removal of Organic Pollutants and Its Environmental-Friendly Regeneration by Peroxydisulfate Process. *Chem. Eng. J.* **2021**, *414*, 128931.

(31) Nakajima, T.; Kurokawa, T.; Ahmed, S.; Wu, W.; Gong, J. Characterization of Internal Fracture Process of Double Network Hydrogels under Uniaxial Elongation. *Soft Matter* **2013**, *9*, 1955-1966.

(32) Gong, J. Why Are Double Network Hydrogels So Tough? *Soft Matter* **2010**, *6*, 2583-2590.

(33) Patel, A. K.; Bajpai, R.; Keller, J. M. On the Crystallinity of PVA/Palm Leaf Biocomposite Using DSC and XRD Techniques. *Microsyst. Technol.* **2014**, *20*, 41-49.

(34) Peppas, N. A.; Merrill, E. W. Differential Scanning Calorimetry of Crystallized PVA Hydrogels. *J. Appl. Polym. Sci.* **1976**, *20*, 1457-1465.

(35) Panigrahi, R.; Chakraborty, S.; Ye, J.; Lim, G. S.; Lim, F. C. H.; Yam, J. K. H.; Wu, L. Y.; Chng, S.; Prawirasatya, M.; van Herk, A. M.; Thoniyot, P. Elucidating the Role of Interfacial Hydrogen Bonds on Glass Transition Temperature Change in a Poly(vinyl alcohol)/SiO_2 Polymer-Nanocomposite by Noncovalent Interaction Characterization and Atomistic Molecular Dynamics Simulations. *Macromol. Rapid Commun.* **2020**, *41*, 2000240.

(36) Liu, P.; Chen, W.; Liu, C.; Tian, M.; Liu, P. A Novel Poly(vinyl alcohol)/Poly(ethylene

glycol) Scaffold for Tissue Engineering with a Unique Bimodal Open-Celled Structure Fabricated Using Supercritical Fluid Foaming. *Sci. Rep.* **2019**, *9*, 9534.

(37) Chen, Y.; Jiao, C.; Peng, X.; Liu, T.; Shi, Y.; Liang, M.; Wang, H. Biomimetic Anisotropic Poly(vinyl alcohol) Hydrogels with Significantly Enhanced Mechanical Properties by Freezing-Thawing under Drawing. *J. Mater. Chem. B* **2019**, *7*, 3243-3249.

(38) Vishwas, M.; Gowda, K. V. A.; Gandla, S. B. Fabrication and Characterization of Fe Doped PVA Films for Optoelectronics. *Mater. Today:. Proc.* **2022**, *68*, 623-627.

(39) Li, L.; Xu, X.; Liu, L.; Song, P.; Cao, Q.; Xu, Z.; Fang, Z.; Wang, H. Water Governs the Mechanical Properties of Poly(vinyl alcohol). *Polymer* **2021**, *213*, 123330.

(40) Hodge, R. M.; Bastow, T. J.; Edward, G. H.; Simon, G. P.; Hill, A. J. Free Volume and the Mechanism of Plasticization in Water-Swollen Poly(vinyl alcohol). *Macromolecules* **1996**, *29*, 8137-8143.

(41) Gu, P.; Li, B.; Wu, B.; Wang, J.; Müller-Buschbaum, P.; Zhong, Q. Controlled Hydration, Transition, and Drug Release Realized by Adjusting Layer Thickness in Alginate-Ca^{2+}/Poly(N-isopropylacrylamide) Interpenetrating Polymeric Network Hydrogels on Cotton Fabrics. *ACS Biomater. Sci. Eng.* **2020**, *6*, 5051-5060.

(42) Hu, N.; Chen, C.; Tan, J.; Wang, W.; Wang, C.; Fan, H.; Wang, J.; Müller-Buschbaum, P.; Zhong, Q. Enhanced Adsorption of Methylene Blue Triggered by the Phase Transition of Thermoresponsive Polymers in Hybrid Interpenetrating Polymer Network Hydrogels. *ACS Appl. Polym. Mater.* **2020**, *2*, 3674-3684.

(43) Hu, N.; Lin, L.; Tan, J.; Wang, W.; Lei, L.; Fan, H.; Wang, J.; Müller-Buschbaum, P.; Zhong, Q. Wearable Bracelet Monitoring the Solar Ultraviolet Radiation for Skin Health

Based on Hybrid IPN Hydrogels. *ACS Appl. Mater. Interfaces* **2020**, *12*, 56480-56490.

(44) Holloway, J. L.; Lowman, A. M.; Palmese, G. R. The Role of Crystallization and Phase Separation in the Formation of Physically Cross-Linked PVA Hydrogels. *Soft Matter* **2013**, *9*, 826-833.

(45) Liu, K.; Han, L.; Tang, P.; Yang, K.; Gan, D.; Wang, X.; Wang, K.; Ren, F.; Fang, L.; Xu, Y.; Lu, Z.; Lu, X. An Anisotropic Hydrogel Based on Mussel-Inspired Conductive Ferrofluid Composed of Electromagnetic Nanohybrids. *Nano Lett.* **2019**, *19*, 8343-8356.

(46) Qian, C.; Higashigaki, T.; Asoh, T.-A.; Uyama, H. Anisotropic Conductive Hydrogels with High Water Content. *ACS Appl. Mater. Interfaces* **2020**, *12*, 27518-27525.